Dalton Transactions

ROYAL SOCIETY OF CHEMISTRY

PAPER

Published on 13 August 2026

Cite this: DOI: 10.1039/d6dt01714b

Thermodynamic description of the $UO_2(NO_3)_2$-$NaNO_3$-H_2O and $UO_2(NO_3)_2$-$Mg(NO_3)_2$-H_2O systems. Solubility experiments and full dissociation Pitzer models

F. Häusler, *[a] A. Lassin,*[b] X. Gaona, [a] A. Prein,[a] F. Greb,[a] N. Cevirim-Papaioannou,[a] P. F. dos Santos, [a] M. Altmaier[a] and B. Madé[c]

Received 13th July 2026,
Accepted 12th August 2026

DOI: 10.1039/d6dt01714b

rsc.li/dalton

The present work improves the understanding on uranium(VI) nitrate systems in acidic, moderate to high ionic strength conditions. Undersaturation solubility studies with the systems $UO_2(NO_3)_2$-$NaNO_3$-H_2O and $UO_2(NO_3)_2$-$Mg(NO_3)_2$-H_2O were conducted at T = (22 ± 0.2) °C. Corresponding solid phases $UO_2(NO_3)_2{\cdot}6H_2O$, $NaNO_3$, and $Mg(NO_3)_2{\cdot}6H_2O$ were identified *via* X-ray powder diffraction. Experimental results are compared with literature data available for the ternary systems at T = 25 °C and indicate a strong dependence on temperature. Based on solubility and isopiestic data, an updated Pitzer model assuming the full dissociation of all involved salts is derived, including new Pitzer interaction parameters $\theta_{UO_2^{2+},Na^+}$, $\theta_{UO_2^{2+},Mg^{2+}}$, $\Psi_{UO_2^{2+},Na^+,NO_3^-}$, and $\Psi_{UO_2^{2+},Mg^{2+},NO_3^-}$. The geochemical code PhreeSCALE was used together with the PhreeSCALE database and the parameter estimation software PEST.

Introduction

Uranium plays a major role in the nuclear fuel cycle and is consequently also highly relevant in the context of radioactive waste disposal. Due to its long half-life (^{238}U: $t_{1/2} = 4.47 \times 10^9$ a, ^{235}U: $t_{1/2} = 7.04 \times 10^8$ a, and ^{236}U: $t_{1/2} = 2.34 \times 10^7$ a),[1] a fundamental understanding of its thermodynamic behaviour for a variety of boundary conditions is essential for long-term safety assessment of radioactive waste repositories. Uranium is known to be stable in oxidation states +IV under strongly reducing conditions and the generally more mobile +VI under weakly reducing to oxidizing conditions.[1–3]

The use of nitric acid in reprocessing activities results in high nitrate inventories in specific streams of low and intermediate level radioactive waste.[4–9] In general, nitrate salts are highly soluble,[10–13] which can potentially lead to aqueous solutions of high ionic strength. Nitrate can locally impact the redox boundary conditions (*i.e.*, acting as oxidizing agent, potentially driving the transition from U(IV) to U(VI)), but can also alter radionuclide speciation through complexation and ion–ion interaction phenomena.

Consequently, the present work focuses on the thermodynamic behaviour of two ternary uranium(VI)-nitrate systems, namely $UO_2(NO_3)_2$-$NaNO_3$-H_2O and $UO_2(NO_3)_2$-$Mg(NO_3)_2$-H_2O. The pH is adjusted acidic to focus on the highly soluble nitrate phases and avoid hydrolysis and carbonate complexation which would be expected to dominate the systems under alkaline conditions. Few comprehensive data sets on uranyl nitrate solubility[14,15] are published to date, which do not provide information on experimental uncertainty or details on solid phase characterization. Because solid phases are integral components of the chemical equilibrium governing solubility, unequivocal identification of the solid phases under the investigated boundary conditions is essential in solubility studies.

In the context of long-term assessment, thermodynamic models based on experimental data need to be determined to properly describe the chemical behaviour. The choice of the Pitzer approach[16,17] enables the description of complex systems up to high ionic strength and is an established basis in reference thermodynamic databases.[18,19] Thermodynamic and activity models of this work are derived on the basis of the full dissociation approach, which limits the number of required interaction parameters, minimizes the risk of overparameterization, and enables the description of experimental data without knowledge on the aqueous speciation beyond the main cations (UO_2^{2+}, Na^+, Mg^{2+}) and anions (NO_3^-).

[a]*Institute for Nuclear Waste Disposal, Karlsruhe Institute of Technology, Karlsruhe, Germany. E-mail: felix.haeusler@kit.edu*
[b]*BRGM, F-45060 Orléans, France. E-mail: a.lassin@brgm.fr*
[c]*Scientific and Technical Division, Andra, Châtenay-Malabry, France*

This work aims to identify and complement relevant experimental data sets of the $UO_2(NO_3)_2$-$NaNO_3$-H_2O and $UO_2(NO_3)_2$-$Mg(NO_3)_2$-H_2O systems and provide ternary Pitzer interaction parameters for an improved thermodynamic description.

Experimental

Chemicals

Solutions were prepared with ultrapure water, purified with a Milli-Q Academic apparatus (Merck Millipore, 18.2 MΩ cm, 22 ± 2 °C, pore size: 0.22 μm). Anhydrous sodium nitrate ($NaNO_3$, p.a., 99 wt%) and magnesium nitrate hexahydrate ($Mg(NO_3)_2{\cdot}6H_2O$, p.a., 99 wt%) were purchased from Thermo Fisher Scientific. Furthermore, uranyl nitrate hexahydrate ($UO_2(NO_3)_2{\cdot}6H_2O$, p.a., Chemapol) from the inventory of KIT-INE was used. Nitric acid (HNO_3 60%, Ultrapur, VWR Chemicals) and perchloric acid ($HClO_4$ 70%, p.a., ITW Reagents) were used for acidification.

Solubility experiments

Independent batch experiments from undersaturation conditions were performed with two series (18 samples total) for the systems $UO_2(NO_3)_2$-$NaNO_3$-H_2O and $UO_2(NO_3)_2$-$Mg(NO_3)_2$-H_2O at T = (22 ± 0.2) °C in concentration ranges of 0.0–8.1 mol $NaNO_3$ per kg H_2O and 0.0–4.9 mol $Mg(NO_3)_2$ per kg H_2O respectively. The pH ≤ 2 was adjusted with HNO_3 or $HClO_4$ to prevent U(VI) hydrolysis. All samples were subjected to regular agitation until thermodynamic equilibrium was reached, which was assumed after analyses of consecutive samplings showed constant total uranium concentrations. Sampling was performed several times for all samples over a period of at least 4 and up to 26 months. Solid and liquid phases were separated by ultrafiltration (10 kDa ≈ 2 nm, Pall Life Science), followed by the dilution of solutions with HNO_3 (2%) by a factor of 1 : 20 301–1 : 40 401 due to high salt concentrations (two dilution steps, gravimetric dilution). U, Na, and Mg concentrations were consecutively measured *via* ICP-OES (Inductively Coupled Plasma Optical Emission Spectroscopy, PerkinElmer Avio 550 Max) as triplicates. The uncertainty of ICP-OES measurements is usually below 5%. Uncertainties for solubility data depicted in the related figures are calculated as standard deviations of the average of single measurements for each sample.

X-ray powder diffraction (XRPD)

Solid phases were characterized by X-ray powder diffraction (XRPD) with a diffractometer D8 Advance (Bruker AXS) with Lynxeye XE-T detector (1D mode) in Bragg–Brentano set-up using Cu-K_α radiation (the high energy resolution of 380 eV of the detector allows the selection of Cu-K_α radiation without an additional monochromator). A step size of 0.013° 2θ with 0.2 s per step was applied within the scan range of 5–60° 2θ, which results in a time of approx. 15 min per measurement. Samples were usually measured 2–3 consecutive times to identify possible phase changes during measurement time after separation of solids from their mother liquor. All XRPD measurements are presented either in this document, or otherwise in the corresponding SI. Sample preparation for XRPD measurements was kept as short as possible (<10 min) to prevent changes of hygroscopic solids. A fraction of the sample was separated as suspension *via* pipette into a separate sample vial. Crystals were gently crushed within the solution and pipetted onto the sample holder (coated with petroleum jelly to fix the solid sample). Adhesive solution was removed with absorbent paper. The sample holder was closed with an airtight dome to minimize potential phase changes.

Thermodynamic modelling

The present work aims at deriving a robust thermodynamic model which describes solubility phenomena in dilute to concentrated salt solutions. Nitrate salts are in general known for their high solubility.[10–12,20] The Pitzer model[16,17] extends the Debye–Hückel approach[21–23] by terms capable of describing short range interactions up to high ionic strength. This is proven in established thermodynamic reference databases[18,19] and makes this a suitable model approach for the description of the $UO_2(NO_3)_2$-$NaNO_3$-H_2O and $UO_2(NO_3)_2$-$Mg(NO_3)_2$-H_2O systems, in which ionic strength can reach high values, above 10 mol per kg H_2O.

The full dissociation approach for dissolved salts is chosen in the present work to describe solubility[14,15] and isopiestic data.[24] This considers that only the dissociated ions UO_2^{2+}, Na^+, Mg^{2+}, and NO_3^- are present as aqueous species when the corresponding salts are dissolved. This limits the number of parameters needed in the parametrization procedure and therefore minimizes the risk of overparameterization. Thus, the resulting parameters inherently include the possible formation of ionic pairs and complex species (*e.g.*, $UO_2NO_3^+$) in solution, but without quantifying the species distribution. This approach has been extensively used in previous studies[25–32] to describe experimental solubility and isopiestic data.

The deviation from ideal behaviour due to the mentioned interactions can be described with activities a_i (−) of solvent and solutes. To model solubility behaviour and compare experimental data with calculations in this model exercise we use the saturation ratio SR (−):

$$\mathrm{SR} = \frac{\prod_i a_i^{\nu_i}}{K^\circ_{s,0}} \quad (1)$$

with ν_i – the number of ions produced by the total dissociation of electrolyte i and $K^\circ_{s,0}$ – the solubility constant (−) of a given solid phase. To describe isopiestic and osmotic data we calculate and compare osmotic coefficients φ (−) as defined by Dinane:[33]

$$\varphi = -\frac{1000 \ln a_w}{M_w \cdot \sum_i \nu_i m_i} \quad (2)$$

with a_w – water activity, M_w – molar mass of water (18.02 g mol^{-1}), m_i – molality (mol per kg H_2O) of dissolved electrolyte i. A more detailed description on this selection and the derivation of the saturation ratio are given in the recent work of Häusler *et al.*,[28] in which we used the same approach for the description of equivalent Eu(III) systems.

Parametrization procedure

The geochemical calculation code PhreeSCALE[34] and the corresponding PhreeSCALE database[19] were used for all calculations in this work. In order to determine new parameters, PhreeSCALE was further coupled with the parameter estimation software PEST.[35]

With the use of the full dissociation approach, the required parameter set to describe the ternary systems consists of the thermodynamic solubility constants $K^{\circ}_{s,0}$ of all involved solid phases at T = 25 °C as well as binary ($\alpha_{1/2}$, $\beta^{(0)}_{i,j}$, $\beta^{(1)}_{i,j}$, $\beta^{(2)}_{i,j}$, $C^{\varphi}_{i,j}$) and ternary ($\theta_{i,k}$, $\Psi_{i,k,j}$) Pitzer interaction parameters (i and k – cations, j – anion).

The parametrization procedure started with calculations in the binary subsystems. Parameter sets given in the PhreeSCALE database were tested against osmotic coefficient data sets[12,24,36–42] and showed an overall satisfactory description in line with the works of Lach *et al.*[43] and Lassin *et al.*[44] Therefore, the given binary interaction parameters were kept constant during the following process.

Further calculations with the only use of binary interaction parameter did not allow a complete description of the solubility data of the ternary systems $UO_2(NO_3)_2$-$NaNO_3$-H_2O and $UO_2(NO_3)_2$-$Mg(NO_3)_2$-H_2O, which demonstrates the influence of ternary interactions on the non-ideal behaviour and thus the need for ternary interaction parameters to improve the description. Therefore, $\theta_{UO_2^{2+},Na^+}$, $\theta_{UO_2^{2+},Mg^{2+}}$, $\Psi_{UO_2^{2+},Na^+,NO_3^-}$, and $\Psi_{UO_2^{2+},Mg^{2+},NO_3^-}$ were determined in iterative processes on the basis of the available experimental data.[14,15,24]

To compare different model attempts and assess the optimization procedure sigma values, σ, were used to quantify the deviation between the resulting model and the experimental data:

$$\sigma = \sqrt{\frac{\sum_{i=1}^{n} (x(i)_{exp} - x(i)_{calc})^2}{n}} \quad (3)$$

with the experimental and calculated values $x(i)_{exp}$ and $x(i)_{calc}$ for a data point i and n as the number of data points in the respective data set. For saturation ratio (4) and osmotic coefficients (5) this leads to:

$$\sigma = \sqrt{\frac{\sum_{i=1}^{n} (\ln SR(i))^2}{n}} \quad (4)$$

$$\sigma = \sqrt{\frac{\sum_{i=1}^{n} (\varphi(i)_{exp} - \varphi(i)_{calc})^2}{n}} \quad (5)$$

Results and discussion

Solubility data

Experimental solubility data determined in this work for the systems $UO_2(NO_3)_2$-$NaNO_3$-H_2O and $UO_2(NO_3)_2$-$Mg(NO_3)_2$-H_2O at T = (22 ± 0.2) °C are listed in Table 1.

Starting with the binary system $UO_2(NO_3)_2$-H_2O, the determined solubility of $UO_2(NO_3)_2{\cdot}6H_2O$ in water of 2.99 ± 0.09 mol per kg H_2O is in good agreement with literature values at 20 °C of 2.98–3.03 mol per kg H_2O,[10,45] and slightly lower than the 25 °C values of 3.21–3.24 mol per kg H_2O.[10,14]

In general, a distinct temperature dependency for the solubility of the investigated nitrate salts can be expected, as illustrated by application of the van't Hoff equation (6):

$$\ln\left(\frac{K_{295.15\,K}}{K_{298.15\,K}}\right) = \frac{\Delta_R H^{\circ}}{R} \cdot \left(\frac{1}{298.15\,K} - \frac{1}{295.15\,K}\right) \quad (6)$$

with solubility constants K at different temperatures, the standard reaction enthalpy $\Delta_R H^{\circ}$ for the dissolution of the salt of interest (calculated based on standard formation enthalpies listed in the NBS tables[46]) and the universal gas constant R = 8.314 J (mol K)$^{-1}$. Calculations result in solubility differences of 0.10 mol per kg H_2O ($UO_2(NO_3)_2{\cdot}6H_2O$), 0.14 mol per kg H_2O ($Mg(NO_3)_2{\cdot}6H_2O$), and 0.49 mol per kg H_2O ($NaNO_3$) when going from 25 °C to 22 °C. A more detailed overview of these calculations is provided in the SI of this work. Although experimental uncertainties have their influence as well, which is also illustrated in the SI, the systematically lower solubilities determined in this work for both ternary series at T = (22 ± 0.2) °C compared to the 25 °C series determined by Colani[14] for $UO_2(NO_3)_2$-$NaNO_3$-H_2O and Yakimov and Nosova[15] for $UO_2(NO_3)_2$-$Mg(NO_3)_2$-H_2O are qualitatively in line with the expected temperature dependence effect.

Table 1 Solubility data and solid phase characterization of this work for the systems $UO_2(NO_3)_2$-$NaNO_3$-H_2O and $UO_2(NO_3)_2$-$Mg(NO_3)_2$-H_2O at T = (22 ± 0.2) °C and pH ≤ 2

$m(NaNO_3)$ in mol per kg H_2O	$m(UO_2(NO_3)_2)$ in mol per kg H_2O	XRPD sample	Solid phase
$UO_2(NO_3)_2$-$NaNO_3$-H_2O			
0	2.99 ± 0.09		
0.70 ± 0.08	2.94 ± 0.17	Na-1	$UO_2(NO_3)_2{\cdot}6H_2O$
2.14 ± 0.17	2.68 ± 0.22		
3.75 ± 0.30	2.42 ± 0.15	Na-2	$UO_2(NO_3)_2{\cdot}6H_2O$
3.84 ± 0.26	2.42 ± 0.15		
4.30 ± 0.26	1.76 ± 0.09		
6.31 ± 0.33	0.89 ± 0.03	Na-3	$NaNO_3$
6.58 ± 0.66	0.95 ± 0.10		
8.14 ± 0.34	0.46 ± 0.01	Na-4	$NaNO_3$
$UO_2(NO_3)_2$-$Mg(NO_3)_2$-H_2O			
0.56 ± 0.04	2.41 ± 0.08	Mg-1	$UO_2(NO_3)_2{\cdot}6H_2O$
1.49 ± 0.09	2.42 ± 0.08	Mg-2	$UO_2(NO_3)_2{\cdot}6H_2O$
1.66 ± 0.15	1.83 ± 0.09		
3.06 ± 0.08	0.91 ± 0.04	Mg-3	$UO_2(NO_3)_2{\cdot}6H_2O$
3.79 ± 0.24	0.83 ± 0.04		
4.65 ± 0.20	0.52 ± 0.04		
4.69 ± 0.30	0.77 ± 0.04		
4.78 ± 0.32	0.64 ± 0.03	Mg-4	$Mg(NO_3)_2{\cdot}6H_2O$
4.93 ± 0.36	0.25 ± 0.02	Mg-5	$Mg(NO_3)_2{\cdot}6H_2O$

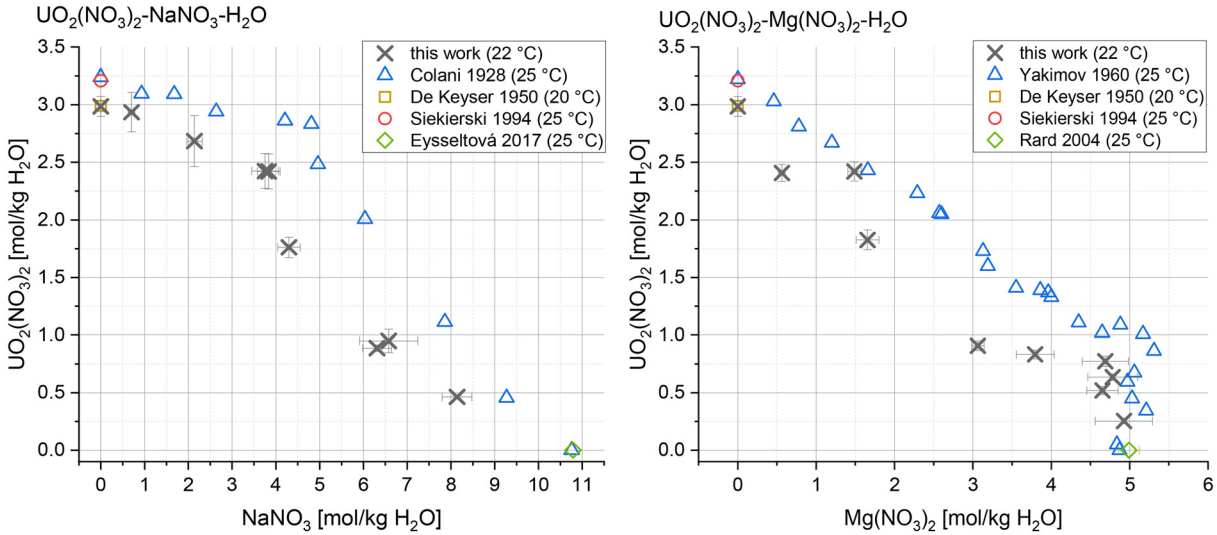

Fig. 1 Solubility data for the system $UO_2(NO_3)_2$-$NaNO_3$-H_2O (left) and $UO_2(NO_3)_2$-$Mg(NO_3)_2$-H_2O (right) of this work at T = (22 ± 0.2) °C (black crosses), compared to literature data at T = 20–25 °C (open symbols).[10–12,14,15,45]

As shown in Fig. 1, the gradual addition of $NaNO_3$ to the $UO_2(NO_3)_2$-H_2O system leads to a decrease in $UO_2(NO_3)_2$ concentration, while the continuous curve progression indicates that $UO_2(NO_3)_2{\cdot}6H_2O$ remains the solid phase in equilibrium. The progression of the resulting solubility curve in the system $UO_2(NO_3)_2$-$NaNO_3$-H_2O changes distinctly above a $NaNO_3$ concentration of 3.8 mol per kg H_2O indicating an invariant point of $UO_2(NO_3)_2{\cdot}6H_2O$ and $NaNO_3$ around 4 molal $NaNO_3$ (comparable to the invariant point identified based on the data of Colani[14] at 25 °C at 4.8 molal $NaNO_3$ and 2.8 molal $UO_2(NO_3)_2$). This phase change is in line with the XRPD characterization of solid phases in equilibrium (see Table 1). Accordingly, starting from the binary system $NaNO_3$–H_2O, nitratine ($NaNO_3$) solubility is reduced by increasing $UO_2(NO_3)_2$ concentration until the described invariant point is reached, at which both $UO_2(NO_3)_2{\cdot}6H_2O$ and $NaNO_3$ are the solid phases in equilibrium with the solution.

For the $UO_2(NO_3)_2$-$Mg(NO_3)_2$-H_2O system, $UO_2(NO_3)_2$ molality decreases almost linearly from 3.0 mol per kg H_2O to 0.8 mol per kg H_2O in the range of 0–4 molal $Mg(NO_3)_2$ with $UO_2(NO_3)_2{\cdot}6H_2O$ remaining the solid phase in equilibrium, which fits the trend observed by Yakimov and Nosova.[15] Their data at 25 °C even describe $UO_2(NO_3)_2{\cdot}6H_2O$ as equilibrium phase up to an invariant point with $Mg(NO_3)_2{\cdot}6H_2O$ at 5.3 mol $Mg(NO_3)_2$ per kg H_2O, followed by a decrease in $Mg(NO_3)_2$ molality to 4.9 mol per kg H_2O as saturation concentration in the binary system $Mg(NO_3)_2$–H_2O. Results of this work indicate the phase change from $UO_2(NO_3)_2{\cdot}6H_2O$ to $Mg(NO_3)_2{\cdot}6H_2O$ in the range of 4.0–4.5 molal $Mg(NO_3)_2$ based on the solubility curve progression and XRPD results. Further solid phases were not observed.

Despite the deviation in absolute values due to temperature dependency effects and potential experimental uncertainties, the experimental solubility series of this work confirm concentration dependent trends seen in the literature data sets of Colani[14] and Yakimov and Nosova,[15] which are to the best of our knowledge so far the only comprehensive solubility data sets over the whole concentration range at T = 25 °C of the systems $UO_2(NO_3)_2$-$NaNO_3$-H_2O and $UO_2(NO_3)_2$-$Mg(NO_3)_2$-H_2O. Comparable solubility curve progressions and stability ranges of the solid equilibrium phases, which are the simple salts $UO_2(NO_3)_2{\cdot}6H_2O$, $NaNO_3$, and $Mg(NO_3)_2{\cdot}6H_2O$, verify findings of these early works and allow reasonable predictions on the thermodynamic behaviour at room temperature. However, downsides of the literature data sets are the missing experimental uncertainties, which impedes a definite evaluation of the data quality, and no information given on how the solid phase characterization was conducted in their work.

Solid phase characterization

Solid phase characterization of selected samples was conducted with X-ray powder diffraction to identify salts in equilibrium with the solutions of the solubility series. An assignment of the solid samples investigated to their respective solution is given in Table 1, while representative XRPD patterns are comparatively shown in Fig. 2 and 3. A summary of all XRPD measurements conducted is given in the SI of this work.

For the $UO_2(NO_3)_2$-$NaNO_3$-H_2O system (Fig. 2), comparison with reference data confirms that $UO_2(NO_3)_2{\cdot}6H_2O$ is the solid phase controlling the solubility in samples Na-1 and Na-2, both with $NaNO_3$ solution concentrations below 4 molal. This observation is in line with the progression of the solubility curve described in the previous section. Accordingly, diffraction patterns of samples Na-3 and Na-4 (with $NaNO_3$ molalities above 4 mol per kg H_2O) are dominated by an intense reflection at approx. 29.5° 2θ, which corresponds to the main reflection line of $NaNO_3$ at 29.7° 2θ.[47] The solid phase $Na[UO_2(NO_3)_3]$ synthesised and characterized by Bäcker and Mudring[48] was not observed in the course of this work, indicating that it is not a stable phase in the thermodynamic

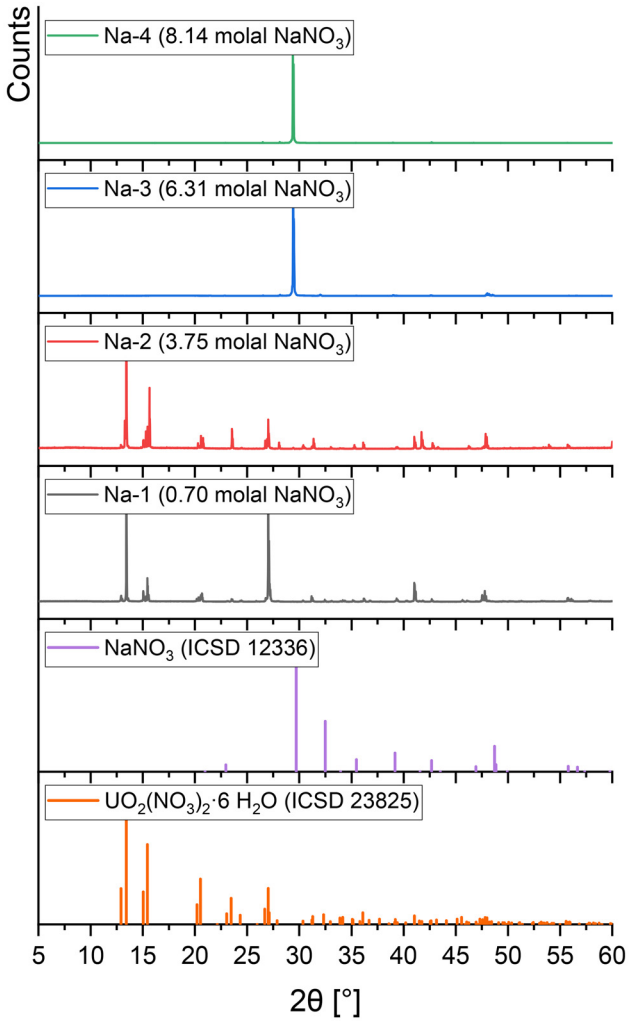

Fig. 2 X-ray powder diffraction patterns of the solid phases Na-1–4 from solubility investigations in the system $UO_2(NO_3)_2$-$NaNO_3$-H_2O (0–8.1 mol $NaNO_3$ per kg H_2O) compared to reference lines.[47,49]

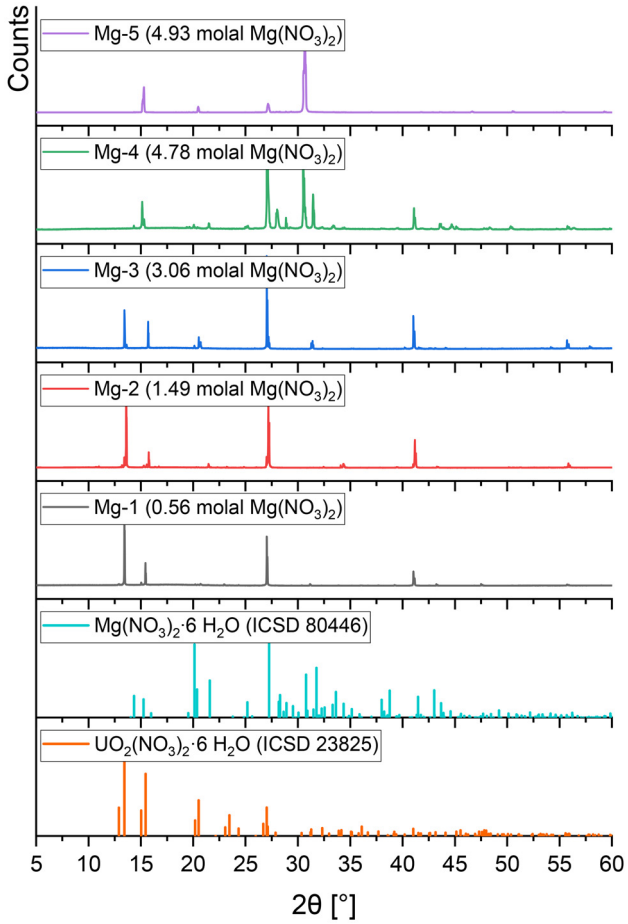

Fig. 3 X-ray powder diffraction patterns of the solid phases Mg-1–5 from solubility investigations in the system $UO_2(NO_3)_2$-$Mg(NO_3)_2$-H_2O (0–4.9 mol $Mg(NO_3)_2$ per kg H_2O) compared to reference lines.[49,50]

solid–liquid-equilibria under the given conditions, which is in line with conclusions by Colani[14] on the basis of solubility data. Note that Bäcker and Mudring[48] synthesized $Na[UO_2(NO_3)_3]$ by dissolving equimolar amounts of UO_3 and $NaNO_3$ in nitric acid solution and allowing isothermal evaporation until single crystals were formed.

The XRPD patterns of samples Mg-1–5 of the $UO_2(NO_3)_2$-$Mg(NO_3)_2$-H_2O system are shown in Fig. 3. Solid phases Mg-1–3 can, based on their respective patterns, clearly be attributed to $UO_2(NO_3)_2{\cdot}6H_2O$, which can best be seen for the recurring reflections at 13.4° 2θ, 15.5° 2θ, and 27.0° 2θ. For samples Mg-4 and Mg-5 in $Mg(NO_3)_2$ rich solutions slightly below 5 molal, $Mg(NO_3)_2{\cdot}6H_2O$ is identified as solid phase, as confirmed by the signals at approx. 15.2° 2θ, 27.2° 2θ and 30.7° 2θ.

XRPD measurements provided some experimental challenges. Comparatively short measurements of roughly crushed crystals for qualitative analyses of the solid phases were performed, to prevent secondary phase changes during sample preparation and measurement. Because of this approach, slight signal displacements and missing features due to preferential crystal orientations were observed. Nonetheless, the results indicate quite clearly the solid equilibrium phases for the investigated samples and verify the conclusions drawn from the evaluation of the solubility data.

Thermodynamic modelling

Parameters selected for the full dissociation Pitzer models of the ternary systems $UO_2(NO_3)_2$-$NaNO_3$-H_2O and $UO_2(NO_3)_2$-$Mg(NO_3)_2$-H_2O are listed in Table 2. Binary Pitzer interaction parameters and solubility constants of $UO_2(NO_3)_2{\cdot}6H_2O$, $NaNO_3$, and $Mg(NO_3)_2{\cdot}6H_2O$ at T = 25 °C were selected as already implemented in the PhreeSCALE database.[19] Binary parameters were comprehensively tested by recalculating osmotic and activity coefficients as in the works of Lach *et al.*[43] and Lassin *et al.*[44] and therefore provide a robust basis for model attempts in more complex systems.

In this work, additional ternary interaction parameters $\theta_{i,k}$ and $\Psi_{i,k,j}$ were determined to improve the description of solubility data at 25 °C by Colani[14] ($UO_2(NO_3)_2$-$NaNO_3$-H_2O) and Yakimov and Nosova[15] ($UO_2(NO_3)_2$-$Mg(NO_3)_2$-H_2O) as well as

Table 2 Pitzer parameters and solubility constants selected for modelling the systems $UO_2(NO_3)_2$-$NaNO_3$-H_2O and $UO_2(NO_3)_2$-$Mg(NO_3)_2$-H_2O at 25 °C in this work

Pitzer parameters binary systems

Species i	Species j	α_2	$\beta^{(0)}_{i,j}$	$\beta^{(1)}_{i,j}$	$\beta^{(2)}_{i,j}$	$C^{\phi}_{i,j}$	Reference
UO_2^{2+}	NO_3^-	0.2562	0.5516	1.4407	−0.0861	−0.0476	Lassin *et al.*[44]
Na^+	NO_3^-	—	0.0038	0.1835	—	0	Lach *et al.*[43]
Mg^{2+}	NO_3^-	—	0.3286	1.9159	—	−0.0064	Lach *et al.*[43]

Pitzer parameters ternary systems

Species i	Species j	Species k	$\theta_{i,k}$	$\Psi_{i,k,j}$	Reference
UO_2^{2+}	NO_3^-	Na^+	−0.0522	0.0126	This work
UO_2^{2+}	NO_3^-	Mg^{2+}	−0.2053	0.0206	This work

Solubility constants

Solid phase	$\log K^{\circ}_{s,0}$	Reference
$UO_2(NO_3)_2{\cdot}6H_2O \rightleftarrows UO_2^{2+} + 2NO_3^- + 6H_2O$	2.2800	Lassin *et al.*[44]
$NaNO_3 \rightleftarrows Na^+ + NO_3^-$	1.0864	Lach *et al.*[43]
$Mg(NO_3)_2{\cdot}6H_2O \rightleftarrows Mg^{2+} + 2NO_3^- + 6H_2O$	3.05	Lach *et al.*[43]

the isopiestic data set for the $UO_2(NO_3)_2$-$NaNO_3$-H_2O system provided by Kirgintsev and Luk'yanov[24] at 25 °C and water activities $0.7543 \leq a_w \leq 0.8969$.

Fig. 4 illustrates the comparison of experimental data and model calculations for the $UO_2(NO_3)_2$-$NaNO_3$-H_2O system at 25 °C. Isopiestic data by Kirgintsev and Luk'yanov[24] are well described with a sigma value of 0.014. Furthermore, the small sigma value of 0.056 for the solubility data indicates an excellent match of experimental results and the introduced model as well. The calculated solubility curves of $UO_2(NO_3)_2{\cdot}6H_2O$ (black) and $NaNO_3$ (red) intercept close to the invariant point of both solid phases stated in the IUPAC solubility data series,[10] which confirms the satisfactory description of the ternary system. Minor deviation can still be observed between

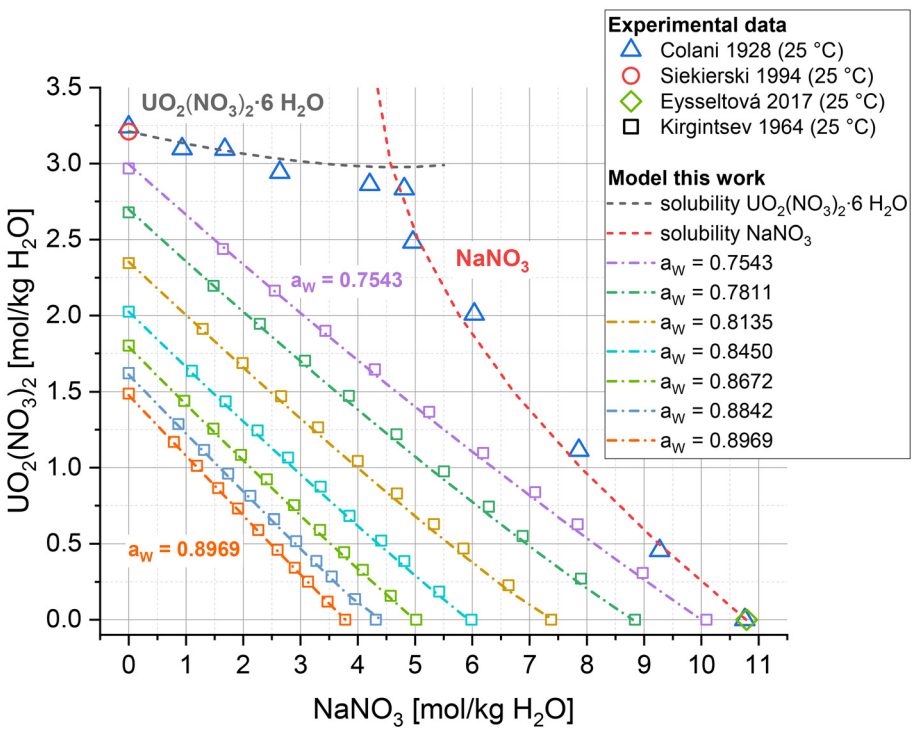

Fig. 4 Solubility and isopiestic literature data for the system $UO_2(NO_3)_2$-$NaNO_3$-H_2O at 25 °C (symbols)[10,11,14,24] compared to corresponding model calculations of this work (lines).

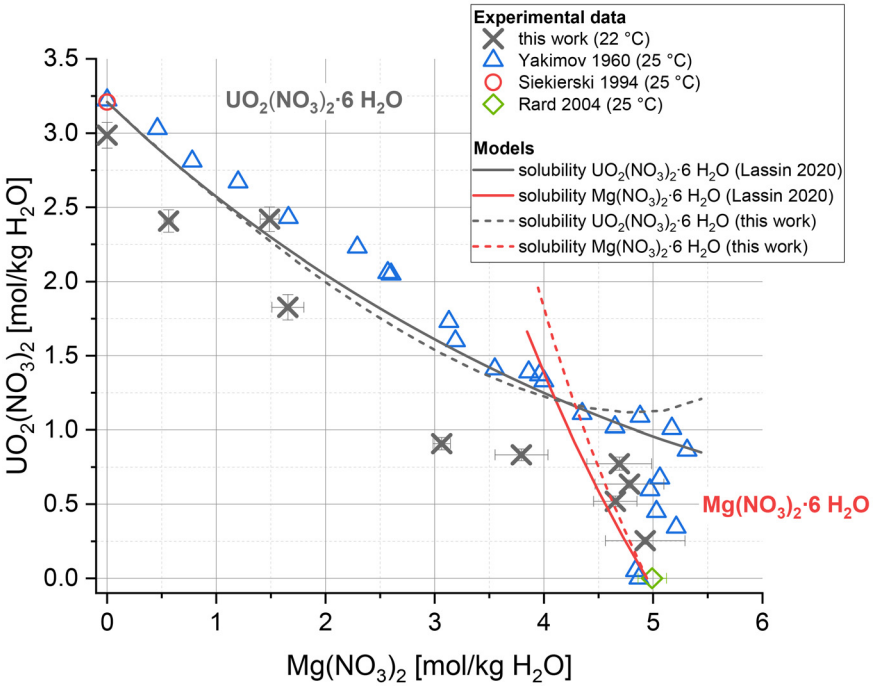

Fig. 5 Solubility data for the system $UO_2(NO_3)_2$-$NaNO_3$-H_2O at 22 °C (this work; black crosses) and 25 °C (open symbols)[10,11,15] compared to corresponding model calculations of Lassin *et al.*[44] (solid lines) and this work (dashed lines).

Colani's data[14] and the proposed model. This is expectedly within the experimental error of solubility measurements, which is unfortunately not stated for the experimental data set.

The PhreeSCALE database already implemented a set of ternary parameters ($\theta_{UO_2^{2+},Mg^{2+}} = -0.5$ and $\Psi_{UO_2^{2+},Mg^{2+},NO_3^-} = 0.07$) for the $UO_2(NO_3)_2$-$Mg(NO_3)_2$-H_2O system based on the work of Lassin *et al.*[44] for which they focused the model exercise on describing Yakimov and Nosova's data (Fig. 5, blue triangles)[15] on the $UO_2(NO_3)_2{\cdot}6H_2O$-branch of the solubility curve (full black line). Attempts to describe the unusual $Mg(NO_3)_2{\cdot}6H_2O$-branch curve progression indicated by the data below 1 molal $UO_2(NO_3)_2$ usually worsen the fit on the rest of the set distinctly. It is unclear how accurate the given data set at 25 °C is, due to missing information on experimental uncertainty. Since Yakimov and Nosova's analytical method for determining solution compositions involved several extraction steps followed by precipitation, a noticeable uncertainty should be assumed, as indicated by the scattering within the data set.

The present work aimed to improve the description in the ternary system at high $Mg(NO_3)_2$ molality. The newly determined solubility data (Fig. 5, black crosses) suggest that a slope steeper than currently described by Lassin's model is indeed expected for the $Mg(NO_3)_2{\cdot}6H_2O$ solubility curve. Attempts to improve the model description in that direction are accompanied a non-monotonous variation in the $UO_2(NO_3)_2{\cdot}6H_2O$-solubility curve with $Mg(NO_3)_2$ molality, which quickly worsens the overall fitting result. Therefore, the best result of our model exercise with ternary parameters $\theta_{UO_2^{2+},Mg^{2+}} = -0.2053$ and $\Psi_{UO_2^{2+},Mg^{2+},NO_3^-} = 0.0206$ (Fig. 5, dashed lines) remains close to the model of Lassin *et al.*[44] (sigma value of 0.342 for the description of solubility data at 25 °C of Yakimov and Nosova[15]). Future work is warranted to generate new and complete solubility data sets at 25 °C, and to further constrain the solution properties by additional investigations within the $UO_2(NO_3)_2$-$Mg(NO_3)_2$-H_2O system *e.g.* by isopiestic or iso-water activity measurements.

Summary and conclusions

Systematic solubility studies on the ternary systems $UO_2(NO_3)_2$-$NaNO_3$-H_2O and $UO_2(NO_3)_2$-$Mg(NO_3)_2$-H_2O were conducted at $T = (22 \pm 0.2)$ °C between 0.0–8.1 mol $NaNO_3$ per kg H_2O and 0.0–4.9 mol $Mg(NO_3)_2$ per kg H_2O in acidic conditions. Corresponding solid phases were identified by X-ray powder diffraction (XRPD). The only solid equilibrium phases identified were $UO_2(NO_3)_2{\cdot}6H_2O$, $NaNO_3$, and $Mg(NO_3)_2{\cdot}6H_2O$. The progression of the determined solubility curves, including identified solids and the observation of invariant points, is in qualitative agreement with literature data at $T = 25$ °C.[14,15] Quantitative deviations are discussed in terms of the noticeable temperature dependency on solubilities of the relevant nitrate salts.

Based on the experimental data available, new ternary Pitzer interaction parameters $\theta_{UO_2^{2+},Na^+}$, $\theta_{UO_2^{2+},Mg^{2+}}$, $\Psi_{UO_2^{2+},Na^+,NO_3^-}$, and $\Psi_{UO_2^{2+},Mg^{2+},NO_3^-}$ were determined to complement established binary data sets in the PhreeSCALE data-

base[19] in order to improve the description of the ternary systems. To do so, the full dissociation assumption was utilized to reduce the number of parameters needed, at the cost of disregarding the formation of any complexes between UO_2^{2+} and NO_3^- in the model description. Since the species distribution in aquatic uranyl nitrate systems is not fully understood by now, future work should be dedicated to systematic spectroscopic studies.

For the $UO_2(NO_3)_2$-$NaNO_3$-H_2O system, the presented full dissociation model describes available solubility and isopiestic data at 25 °C satisfactorily. In case of the $UO_2(NO_3)_2$-$Mg(NO_3)_2$-H_2O system, a complete description of the of the solubility data was not achieved. Further experimental data, especially for the aqueous phase, are needed to verify the present data sets and further constrain the model exercise for a more detailed and robust description of the $UO_2(NO_3)_2$-$Mg(NO_3)_2$-H_2O system.

Conflicts of interest

There are no conflicts to declare.

Data availability

Additional data supporting this article have been included as part of the supplementary information (SI). Supplementary information: utilization of the van't Hoff equation to illustrate temperature dependency effects, additional comparison of solubility data and all XRD measurements. See DOI: https://doi.org/10.1039/d6dt01714b.

Acknowledgements

The present work was realized in the collaborative project co-funded by Andra, BRGM and KIT-INE.

References

1 N. Çevirim-Papaioannou, E. Yalçıntaş, X. Gaona, K. Dardenne, M. Altmaier and H. Geckeis, Redox Chemistry of Uranium in Reducing, Dilute to Concentrated NaCl Solutions, *Appl. Geochem.*, 2018, **98**, 286–300, DOI: 10.1016/j.apgeochem.2018.07.006.

2 X. Gaona, D. A. Kulik, N. Macé and E. Wieland, Aqueous–Solid Solution Thermodynamic Model of U(VI) Uptake in C–S–H Phases, *Appl. Geochem.*, 2012, **27**(1), 81–95, DOI: 10.1016/j.apgeochem.2011.09.005.

3 M. Altmaier, X. Gaona and T. Fanghänel, Recent Advances in Aqueous Actinide Chemistry and Thermodynamics, *Chem. Rev.*, 2013, **113**(2), 901–943, DOI: 10.1021/cr300379w.

4 A. P. Paiva and P. Malik, Recent Advances on the Chemistry of Solvent Extraction Applied to the Reprocessing of Spent Nuclear Fuels and Radioactive Wastes, *J. Radioanal. Nucl. Chem.*, 2004, **261**(2), 485–496, DOI: 10.1023/B:JRNC.0000034890.23325.b5.

5 M. Herm, X. Gaona, T. Rabung, D. Fellhauer, C. Crepin, K. Dardenne, M. Altmaier and H. Geckeis, Solubility and Spectroscopic Study of AnIII/LnIII in Dilute to Concentrated Na–Mg–Ca–Cl–NO_3 Solutions, *Pure Appl. Chem.*, 2015, **87**(5), 487–502, DOI: 10.1515/pac-2014-1205.

6 H. Ma, M. Shen, Y. Tong and X. Wang, Radioactive Wastewater Treatment Technologies: A Review, *Molecules*, 2023, **28**(4), 1935, DOI: 10.3390/molecules28041935.

7 A. Lassin, P. F. dos Santos, X. Gaona, M. Altmaier and B. Madé, Solution and Solid-Liquid-Equilibrium Properties of Radionuclide-Nitrate Aqueous Systems: Experiments and SIT Parameterization, in *Migration 2023*, Nantes, France, 2023.

8 V. Metz, W. Schüßler, B. Kienzler and T. Fanghänel, Geochemically Derived Non-Gaseous Radionuclide Source Term for the Asse Salt Mine – Assessment for the Use of a $Mg(OH)_2$-Based Backfill Material, *Radiochim. Acta*, 2004, **92**(9–11), 819–825, DOI: 10.1524/ract.92.9.819.54991.

9 B. A. Crawford, S. A. Lott, L. D. Sparks, G. Van Soest and B. McInroy, The Road to Recertification: WIPP TRU Waste Inventory, in *Proceedings of Waste Management* 2006 *Conference*, WMS Tempe, AZ, 2006.

10 S. Siekierski, S. L. Phillips and J. D. Navratil, *IUPAC SDS 55 - Actinide Nitrates*, IUPAC Solubility Data Series, Oxford University Press, 1994, vol. 55.

11 J. Eysseltová, V. Zbranek, M. Y. Skripkin, K. Sawada and S. Tepavitcharova, IUPAC-NIST Solubility Data Series. 89. Alkali Metal Nitrates. Part 2. Sodium Nitrate, *J. Phys. Chem. Ref. Data*, 2017, **46**(1), 013103, DOI: 10.1063/1.4972807.

12 J. A. Rard, A. M. Wijesinghe and T. J. Wolery, Review of the Thermodynamic Properties of $Mg(NO_3)_2$(aq) and Their Representation with the Standard and Extended Ion-Interaction (Pitzer) Models at 298.15 K, *J. Chem. Eng. Data*, 2004, **49**(5), 1127–1140, DOI: 10.1021/je049868l.

13 *Scandium, Yttrium, Lanthanum and Lanthanide Nitrates*, ed. S. Siekierski, T. Mioduski and M. Salomon, Solubility data series, Pergamon Press, Oxford New York Toronto Sydney Paris Frankfurt (Main) Kronberg-Taunus, 1st edn, 1983.

14 A. Colani, No 15. - Étude des systémes: nitrate d'uranyle, nitrate alcalin, eau, á 25°, *Bull. Soc. Chim. Fr.*, 1928, **43**, 194–199.

15 M. A. Yakimov and N. F. Nosova, Solubility Isotherm of the $UO_2(NO_3)_2$-$Mg(NO_3)_2$-H_2O System at 0° and 25°, *Russ. J. Inorg. Chem.*, 1960, **5**(3), 346–347.

16 K. S. Pitzer, *Activity Coefficients in Electrolyte Solutions*, CRC Press, Boca Raton, FL, USA, 1991, vol. 2.

17 K. S. Pitzer, Thermodynamics of Electrolytes. I. Theoretical Basis and General Equations, *J. Phys. Chem.*, 1973, **77**(2), 268–277, DOI: 10.1021/j100621a026.

18 THEREDA - Thermodynamic Reference Database, 2024. https://www.thereda.de/.

19 L. André, A. Lassin and A. Lach, *PHREESCALE.DAT: A Thermodynamic Database for the PhreeSCALE Software. Version 1.0*, 2020. DOI: 10.18144/xy83-6848.

20 D. G. Archer, Thermodynamic Properties of the $NaNO_3$+H_2O System, *J. Phys. Chem. Ref. Data*, 2000, **29**(5), 1141–1156, DOI: 10.1063/1.1329317.

21 G. Scatchard, Concentrated Solutions of Strong Electrolytes, *Chem. Rev.*, 1936, **19**(3), 309–327, DOI: 10.1021/cr60064a008.

22 C. E. Harvie and J. H. Weare, The Prediction of Mineral Solubilities in Natural Waters: The Na-K-Mg-Ca-Cl-SO_4-H_2O System from Zero to High Concentration at 25° C, *Geochim. Cosmochim. Acta*, 1980, **44**(7), 981–997, DOI: 10.1016/0016-7037(80)90287-2.

23 J. C. Sohr, *Löslichkeitsgleichgewichte mit Lithiumsalzen und deren Modellierung mit dem Fokus auf das Salar-Brine-System bei tiefen Temperaturen*, TU Bergakademie Freiberg, Freiberg(Sachs), 2022.

24 A. N. Kirgintsev and A. V. Luk'yanov, Study of ternary solutions by an isopiestic method. IV, *Radiokhimiya*, 1964, **6**(4), 449–454.

25 C. Christov and N. Møller, Chemical Equilibrium Model of Solution Behavior and Solubility in the H-Na-K-OH-Cl-HSO_4-SO_4-H_2O System to High Concentration and Temperature, *Geochim. Cosmochim. Acta*, 2004, **68**(6), 1309–1331, DOI: 10.1016/j.gca.2003.08.017.

26 A. Lach, L. André and A. Lassin, Darapskite Solubility in Basic Solutions at 25 °C: A Pitzer Model for the Na-NO_3-SO_4-OH-H_2O System, *Appl. Geochem.*, 2017, **78**, 311–320, DOI: 10.1016/j.apgeochem.2016.12.008.

27 P. F. dos Santos, A. Lassin, X. Gaona, K. Garbev, M. Altmaier and B. Madé, Thermodynamics of the Eu(III)–Mg–SO_4–H_2O and Eu(III)–Na–SO_4–H_2O Systems. Part I: Solubility Experiments and the Full Dissociation Pitzer Model, *Dalton Trans.*, 2024, **53**(14), 6289–6299, DOI: 10.1039/D3DT04322C.

28 F. Häusler, P. F. dos Santos, A. Lassin, X. Gaona, K. Garbev, S. Touzelet, Y. Cartigny, M. Altmaier and B. Madé, Thermodynamic Description of $Eu(NO_3)_3$-$NaNO_3$-H_2O and $Eu(NO_3)_3$-$Mg(NO_3)_2$-H_2O Systems. Solubility Experiments and Full Dissociation Pitzer Models, *RSC Adv.*, 2026, **16**(28), 25927–25943, DOI: 10.1039/D5RA09321J.

29 C. E. Harvie, N. Møller and J. H. Weare, The Prediction of Mineral Solubilities in Natural Waters: The Na-K-Mg-Ca-H-Cl-SO_4-OH-HCO_3-CO_3-CO_2-H_2O System to High Ionic Strengths at 25 °C, *Geochim. Cosmochim. Acta*, 1984, **48**(4), 723–751, DOI: 10.1016/0016-7037(84)90098-X.

30 A. Keller, J. Burger, H. Hasse and M. Kohns, Application of the Pitzer Model for Describing the Evaporation of Seawater, *Desalination*, 2021, **503**, 114866, DOI: 10.1016/j.desal.2020.114866.

31 R. T. Pabalan and K. S. Pitzer, Thermodynamics of Concentrated Electrolyte Mixtures and the Prediction of Mineral Solubilities to High Temperatures for Mixtures in the System Na-K-Mg-Cl-SO_4-OH-H_2O, *Geochim. Cosmochim. Acta*, 1987, **51**(9), 2429–2443, DOI: 10.1016/0016-7037(87)90295-X.

32 D. A. Palmer, J. A. Rard and S. L. Clegg, Isopiestic Determination of the Osmotic and Activity Coefficients of Rb_2SO_4(aq) and Cs_2SO_4(aq) at T = (298.15 and 323.15) K, and Representation with an Extended Ion-Interaction (Pitzer), Model, *J. Chem. Thermodyn.*, 2002, **34**(1), 63–102, DOI: 10.1006/jcht.2000.0901.

33 A. Dinane, Thermodynamic Properties of {NaCl-CsCl-LiCl}(aq) at T=298.15 K: Water Activities, Osmotic and Activity Coefficients, *J. Solution Chem.*, 2007, **36**(11), 1421–1436, DOI: 10.1007/s10953-007-9199-1.

34 A. Lach, F. Boulahya, L. André, A. Lassin, M. Azaroual, J.-P. Serin and P. Cézac, Thermal and Volumetric Properties of Complex Aqueous Electrolyte Solutions Using the Pitzer Formalism – The PhreeSCALE Code, *Comput. Geosci.*, 2016, **92**, 58–69, DOI: 10.1016/j.cageo.2016.03.016.

35 J. Doherty, *PEST Model-Independent Parameter Estimation User Manual*, Watermark Numerical Computing, Brisbane, Australia, 2004, vol. 3338, p. 3349.

36 R. A. Robinson, J. M. Wilson and H. S. Ayling, The Activity Coefficients of Some Bivalent Metal Nitrates in Aqueous Solution at 25° from Isopiestic Vapor Pressure Measurements, *J. Am. Chem. Soc.*, 1942, **64**(6), 1469–1471, DOI: 10.1021/ja01258a064.

37 R. A. Robinson and C. K. Lim, 403. The Osmotic and Activity Coefficients of Uranyl Nitrate, Chloride, and Perchlorate at 25°, *J. Chem. Soc.*, 1951, 1840–1843, DOI: 10.1039/JR9510001840.

38 R. N. Goldberg, Evaluated Activity and Osmotic Coefficients for Aqueous Solutions: Bi-univalent Compounds of Lead, Copper, Manganese, and Uranium, *J. Phys. Chem. Ref. Data*, 1979, **8**(4), 1005–1050, DOI: 10.1063/1.555611.

39 A. Ruas, O. Bernard, B. Caniffi, J.-P. Simonin, P. Turq, L. Blum and P. Moisy, Uranyl(VI) Nitrate Salts: Modeling Thermodynamic Properties Using the Binding Mean Spherical Approximation Theory and Determination of "Fictive" Binary Data, *J. Phys. Chem. B*, 2006, **110**(7), 3435–3443, DOI: 10.1021/jp056733t.

40 Y. C. Wu and W. J. Hamer, Revised Values of the Osmotic Coefficients and Mean Activity Coefficients of Sodium Nitrate in Water at 25 °C, *J. Phys. Chem. Ref. Data*, 1980, **9**(2), 513–518, DOI: 10.1063/1.555621.

41 M. El Guendouzi and M. Marouani, Water Activities and Osmotic and Activity Coefficients of Aqueous Solutions of Nitrates at 25°C by the Hygrometric Method, *J. Solution Chem.*, 2003, **32**(6), 535–546, DOI: 10.1023/A:1025365900350.

42 P. R. Zalupski, R. McDowell and S. L. Clegg, Isopiestic Determination of the Osmotic Coefficients of $NaNO_3$ + $Eu(NO_3)_3$ + H_2O at 298.15 K and Representation with an Extended Ion-Interaction (Pitzer) Model, *J. Chem. Eng. Data*, 2014, **59**(5), 1574–1582, DOI: 10.1021/je500016d.

43 A. Lach, L. André, S. Guignot, C. Christov, P. Henocq and A. Lassin, A Pitzer Parametrization To Predict Solution Properties and Salt Solubility in the H–Na–K–Ca–Mg–NO_3–H_2O System at 298.15 K, *J. Chem. Eng. Data*, 2018, **63**(3), 787–800, DOI: 10.1021/acs.jced.7b00953.

44 A. Lassin, S. Guignot, A. Lach, C. Christov, L. André and B. Madé, Modeling the Solution Properties and Mineral–

Solution Equilibria in Radionuclide-Bearing Aqueous Nitrate Systems: Application to Binary and Ternary Systems Containing U, Th, or Lanthanides at 25 °C, *J. Chem. Eng. Data*, 2020, **65**(7), 3613–3626, DOI: 10.1021/acs.jced.0c00180.

45 W. L. De Keyser, R. Cypres and M. Herrmann, A Contribution to the Study of the Solubility of Uranyl Nitrate in Organic Solvents, *Bull. Cent. Phys. Nucl. Univ. Libre Bruxelles*, 1950, **17**.

46 D. D. Wagman, W. H. Evans, V. B. Parker, R. H. Schumm, I. Halow, S. M. Bailey, K. L. Churney and R. L. Nuttall, The NBS Tables of Chemical Thermodynamic Properties: Selected Values for Inorganic and C_1 and C_2 Organic Substances in SI Units, *J. Phys. Chem. Ref. Data*, 1982, **11**(Supplement 2).

47 Y. V. Nelyubina, A. A. Korlyukov, K. A. Lyssenko and I. V. Fedyanin, Transferable Aspherical Atom Modeling of Electron Density in Highly Symmetric Crystals: A Case Study of Alkali-Metal Nitrates, *Inorg. Chem.*, 2017, **56**(8), 4688–4696, DOI: 10.1021/acs.inorgchem.7b00340.

48 T. Bäcker and A.-V. Mudring, Sodium Trinitratouranylate (VI) $Na[UO_2(NO_3)_3]$, *Z. Anorg. Allg. Chem.*, 2010, **636**(6), 1002–1005, DOI: 10.1002/zaac.201000033.

49 J. C. Taylor and M. H. Mueller, A Neutron Diffraction Study of Uranyl Nitrate Hexahydrate, *Acta Crystallogr.*, 1965, **19**(4), 536–543, DOI: 10.1107/S0365110X65003857.

50 J. Schefer and M. Grube, Low Temperature Structure of Magnesium Nitrate Hexahydrate, $Mg(NO_3)_2{\cdot}6H_2O$: A Neutron Diffraction Study at 173 K, *Mater. Res. Bull.*, 1995, **30**(10), 1235–1241, DOI: 10.1016/0025-5408(95)00122-0.

